5
Detection of Cd^{2+} ions using MPA-GSH functionalized AlGaN/GaN HEMT

In this chapter, an approach was developed to detect cadmium ions by employing AlGaN/GaN HEMT. For this, the fabrication of AlGaN/GaN HEMTs was carried out in a similar way, as explained in chapter 4. Additionally, the gate contact of the fabricated AlGaN/GaN HEMT was functionalized with Mercaptopropionic acid (MPA) and Glutathione (GSH) to detect cadmium ions. The chapter starts with the introduction section, which covers the background information related to cadmium ions. After this, the development of the functionalized layer over the gate terminal is described. Furthermore, the electrical analysis for sensing is discussed. At the end of the chapter, the sensing mechanism of Cd^{2+} ions with AlGaN/GaN HEMT is explained.

5.1 INTRODUCTION

Naturally, heavy metals are commonly present in water and soil. Among several heavy metals, some metals like iron (Fe), cobalt (Co), manganese (Mn), zinc (Zn), and many more are necessary for the life system in small quantities. However, many other heavy metals such that mercury (Hg), lead (Pb), nickel (Ni), arsenic (As), cadmium (Cd), tin (Sn), and chromium (Cr) are not only toxic but can cause cancer and neurodegenerative diseases and can affect liver and kidney functions [Chow *et al.*, 2005]. Metals like Cd, Pb, As, Cr, Hg, are also considered as environmental health hazards at the lower concentration as they ranked in the top 10 toxic metals of the *Agency for Toxic Substances and Disease Registry Priority List of Hazardous Substances* [Gumpu *et al.*, 2015]. The sources of these toxic heavy metals are paints, automobile exhaust, wastes from mining, coal, and other industries [March *et al.*, 2015]. Cadmium is one of the toxic metals that are carcinogens occurring from mining and rubber industries, electroplated parts, batteries, and engraving processes. It can cause fatigue, osteoporosis, kidney dysfunction, weight loss, pulmonary fibrosis, and hypertension [Li *et al.*, 2001]. The standard limit set by the World Health Organization (WHO) for Cd in drinking water is 3 ppb [Organization, 2011] and 5 ppb by the Environmental Protection Agency (EPA) [López Marzo *et al.*, 2013]. It means that below this limit, the quantity of Cd in any form is not harmful to the human body. If it exceeds this permissible quantity, it can cause various health issues, as mentioned above.

The Cd is affecting human health worldwide. In 2014, a report *Status of Trace and Toxic Metals in Indian Rivers* of Central Water Commission, and Ministry of Water Resources, Government of India stated that an observation has been carried out for the status of toxic metals [Directorate, 2014] and found that some rivers where the most population resides have Cd content more than the BIS acceptable limits [Directorate, 2014; Gumpu *et al.*, 2015]. Previously in 2013, the Government of South China conducted a test on the rice samples, and test reports indicated that among them, some samples in South China are contaminated with Cd [Guo *et al.*, 2014]. Since a large population of the world is living in these countries, affected by Cd, therefore, it is desirable to detect Cd to its acceptable limits by highly selective and sensitive methods [Directorate, 2014; Gumpu *et al.*, 2015; Guo *et al.*, 2014].

Different methodologies, e.g., colorimetric, biochemical, electrochemical, and paper-based device approaches [Bansod *et al.*, 2017; Chow *et al.*, 2005; Feng *et al.*, 2015; Guo *et al.*, 2014; Kabir *et al.*, 2018; Kang *et al.*, 2007; López Marzo *et al.*, 2013; Pei *et al.*, 2011] have been used for the

detection of Cd in water. However, these approaches for sensing techniques are excellent under the laboratory environments, but these techniques are not suitable for every environmental condition and different sites. Thus, there is a necessity for small, portable, easy to handle sensing devices having the capability to work with wireless applications in the external environment, and that must have superior qualities such as fast response, reproducible and reliable. Generally, the semiconductor-based sensors are fabricated using silicon as a substrate since the Silicon industry is well matured and dominating in the semiconductor market. However, the Silicon-based sensors are not suitable for harsh environmental conditions, like high temperature and corrosive environment [Chu *et al.*, 2010b; Kang *et al.*, 2008]. $Al_xGa_{1-x}N$/GaN HEMT based sensors are more superior to other portable sensor technologies like silicon because of their properties of having wide bandgaps, high electron mobility, high 2DEG sheet carrier concentration piezoelectric polarization, and availability of surface charge to achieve robustness and high sensitivity [Asadnia *et al.*, 2016; Nigam *et al.*, 2017; Tripathy *et al.*, 2012]. Nowadays, Many researchers are attracted towards AlGaN/GaN HEMT as a sensor for the detection of toxic metals like Hg [Asadnia *et al.*, 2016; Chen *et al.*, 2008; Kang *et al.*, 2007], pH detection [Dong *et al.*, 2018; Jia *et al.*, 2016; Kang *et al.*, 2007; Podolska *et al.*, 2010; Steinhoff *et al.*, 2003], nitrate ions [Myers *et al.*, 2013], biomolecules like glucose[Chai *et al.*, 2010] and DNA hybridization [Thapa *et al.*, 2012], breath analyzer [Chai *et al.*, 2010] and prostate-specific antigen [Wang *et al.*, 2007]. Hence, the AlGaN/GaN HEMT has proved itself for many sensing applications, including bio as well as chemical sensors.

Considering the toxicity of Cd, heavy metals, the Cd appears next to the Hg; hence the device should have the capability to detect the lower concentration of Cd in every environmental condition (including the harsh and corrosive environment) with quick response, high reusability, and good selectivity.

5.2 MATERIALS USED IN THE EXPERIMENT

The materials used in this work are reduced glutathione (99% purity), ethanol, Sodium hydroxide (NaOH), perchloric acid ($HClO_4$), 3-mercaptopropionic acid (MPA), N-hydroxy-succinimide (NHS), ammonium acetate, 2-(N-morpholino)-ethane-sulfonic-acid (MES), copper (II) sulfate, chromium (III) nitrate, cadmium (II) nitrate, nickel (II) nitrate, zinc (II) nitrate, mercury (II) nitrate, lead (II) nitrate, and 1-ethyl-3-(3-dimethyl aminopropyl)-carbodiimide-hydrochloride (EDC). The NaOH and HNO_3 were used for pH adjustment of buffer solutions. The stock solutions of the above chemicals were made in the ammonium acetate solution.

5.3 FUNCTIONALIZATION PROCESS OF MPA AND GSH ON AlGaN/GaN HEMT

The functionalization of the surface of the semiconductor device is necessary for specific and selective detection of chemicals or ions. Devices such as ISFETs and HEMTs can easily differentiate the adsorption of anions and cations and show those changes by incrementing or decrementing the channel conductance. Although, precise detection of a specific type of ions necessitates functionalization of the surface of the device.

The functionalization of MPA–GSH is performed over the gate region of the AlGaN/GaN HEMT, as shown in Figure 5.1. First, the solution of 10 mM MPA was prepared in the mixture of 5 ml water and 15 ml ethanol in which the device was incubated at room temperature for 12 hours. Then the device was rinsed with absolute ethanol. Furthermore, the device was immersed in a continuously stirred solution of 4 mM NHS and 20 mM EDC in 100 mM MES buffer for 1 hour. This process activates the carboxyl terminus on the gate. Subsequently, the device was rinsed with 25 mM MES buffer several times. Finally, the device was immersed in a 50 mg/ml GSH solution (prepared in 100 mM MES buffer) at 4˚C for 12 hours to form MPA-GSH functionalized layer on the gate [Chow *et al.*, 2005; Nigam *et al.*, 2019a].

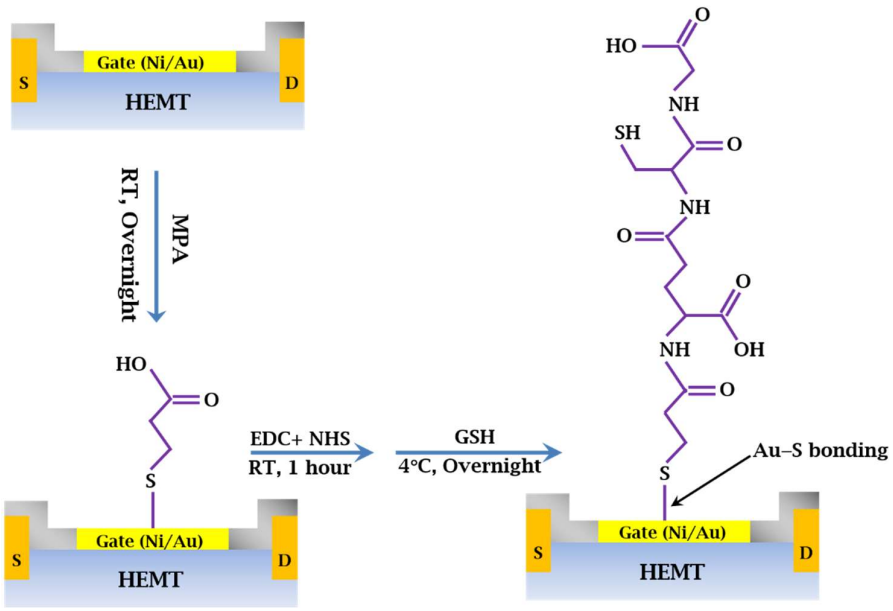

Figure 5.1: Functionalization process of MPA and GSH on Au gate contact of AlGaN/GaN HEMT

5.4 MEASUREMENT AND CHARACTERIZATION

The current-voltage characteristic of the fabricated HEMT device was measured by the Keithley-4200 semiconductor characterization system with the gate region exposed. The detection of the Cd^{2+} ions was observed by measuring the variation in the electrical characteristics of the AlGaN/GaN HEMT sensor. The shift in the I_{DS} (drain current) by keeping fixed V_{DS} (drain to source voltage) at +0.5 V was measured when the gate terminal of the HEMT unveiled to different Cd^{2+} ions concentrations. Solutions were prepared with different Cd^{2+} ion concentrations varying from 0.2 ppb to 10 ppm in 50 mM ammonium acetate buffer.

5.5 REAL-TIME DETECTION OF Cd^{2+} IONS

HEMTs are different from other devices as there is no requirement of intentional doping for charge transport. It possesses unique properties called spontaneous and piezoelectric polarization due to which the two-dimensional electron gas (2DEG) is formed at the hetero-interface of the AlGaN barrier layer and GaN channel layer as shown in Figure 5.2 [Nigam *et al.*, 2017] and has been described previously. The availability of 2DEG makes the device as normally-on as the device possesses the current even at V_{GS}=0. As mentioned earlier, due to the polarization effect, the surface charges are available at the top of the cap layer. Thus, the 2DEG concentration in the channel is highly sensitive to the variation of surface charges or gate potential (V_G) of AlGaN/GaN HEMTs, leading to a change in the drain current (I_{DS}). The drain current (I_{DS}) of standard AlGaN/GaN HEMT can be given by the following expression [Dong *et al.*, 2018]:

$$I_{DS} = \frac{\varepsilon_n \mu W}{2dL}\left[2(V_G - V_T)V_{DS} - V_{DS}^2\right] \tag{5.1}$$

where ε_n is the permittivity of $Al_xGa_{1-x}N$ barrier layer and GaN cap layer, μ is the mobility of the electron in 2DEG, L and W are the length and width of the gate contact respectively, V_G is the gate voltage, V_{DS} is the drain voltage, V_T is the threshold voltage, and d is the distance between the surface and 2DEG. The parameters ε_N, d, W, L, and V_T are constant. The V_{DS} is kept constant while making the gate terminal open to sense the metal ions; the gate-potential variations directly affect the drain current (I_{DS}). The particularity of this HEMT sensor is that there is no need for the reference electrode. Based on the working principle and the AlGaN/GaN HEMT properties, an appropriately functionalized AlGaN/GaN HEMT Cd^{2+} ion sensor is demonstrated.

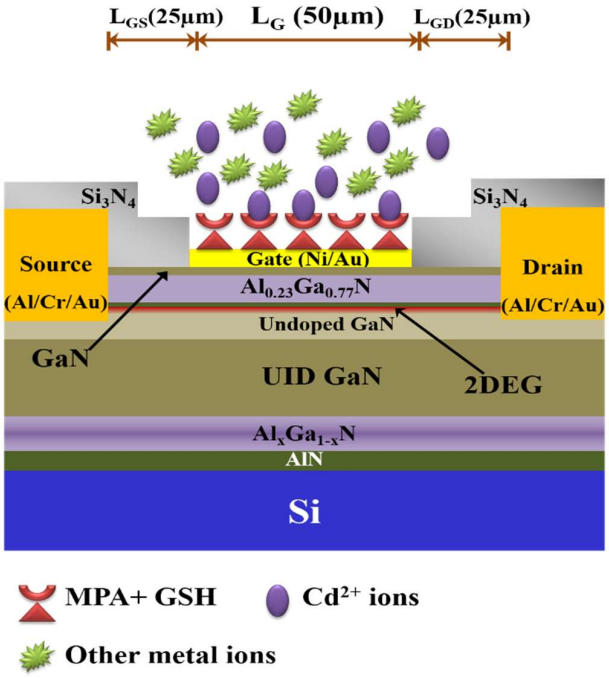

Figure 5.2: The Layered structure of AlGaN/GaN HEMT sensor with the functionalized gate by 3-Mercaptopropionic acid (MPA) and Glutathione (GSH) for detection of Cd^{2+} ions.

Figure 5.3 described the I_{DS} response of the Cd^{2+} ion sensor to the different concentrations of Cd^{2+} ions exposed to the gate contact of AlGaN/GaN HEMT at the fixed drain voltage of +0.5 V. The I_{DS} did not change when deionized water interacts with the sensitive zone of the device. When 1 ppb of Cd^{2+} ion solution interacted with the functionalized surface of the gate, a reduction in current was observed. By the cumulative addition of the Cd^{2+} ion solution, the current decreased [Nigam *et al.*, 2019a]. The characterization of the sensor at each concentration was done until 5 minutes, as shown in Figure 5.3.

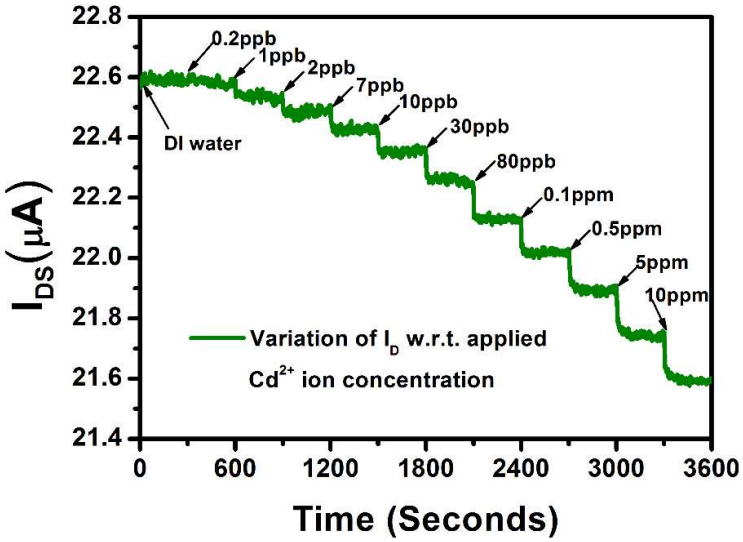

Figure 5.3: Real-time electrical response of AlGaN/GaN HEMT sensor with different Cd^{2+} ion concentrations at V_{DS}= +0.5 V.

The variation in the drain current of the device by exposing the functionalized gate region to the solution with no metal ion concentration (termed as blank) and to 10 ppm Cd^{2+} ion solution

was shown in Figure 5.4. Here, the V_{DS} varied from 0 to 3V, and the corresponding I_{DS} was observed with the interaction of blank and 10 ppm Cd^{2+} ion solution on the functionalized gate region of HEMT. This process explains the decrement of I_{DS} due to the influence of Cd^{2+} ions on the MPA-GSH functionalized gate region.

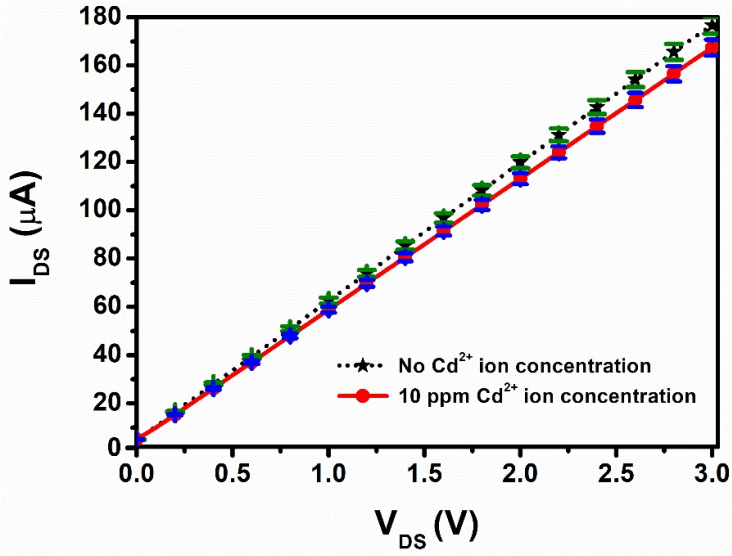

Figure 5.4: I_D-V_D characteristics of the device where its gate was exposed to a 10 ppm Cd^{2+} ion concentration and Cd^{2+} ion free solutions, respectively.

5.6 DETERMINATION OF SENSITIVITY AND LIMIT OF DETECTION

The limit of detection and sensitivity are the essential parameters of the sensors that describe the performance of the sensor. The limit of detection is observed by the 3-sigma approach, which was discussed in chapter 1 and can be given as [Guo *et al.*, 2014; Jia *et al.*, 2016]:

$$LoD = 3\sigma/m \tag{5.2}$$

where σ is the Standard Deviation of the least concentration, and m is the slope of the calibration curve. By performing appropriate calculations for the Eq. (5.2) and by calibration of the curve shown in Figure 5.5, the sensitivity of the sensor was calculated as the slope of the calibration curve (m) and is obtained as 0.241 μA/ppb. The Standard Deviation (σ) determined as 0.0205, the linear regression coefficient of the calibration line (R^2) is 0.9883, and hence the limit of detection (LoD) is obtained as 0.255 ppb, which is sufficiently below the allowed limit of the WHO standard of Cd^{2+} ions in drinking water (0.003 mg/l or 3 ppb) [Nigam *et al.*, 2019a]. The calibration curve was observed by subtracting the average current of a particular concentration from the base current, as shown in Figure 5.5. Here the error bars stand for comparison of experimental data with calibration plot.

5.7 RESPONSE TIME AND SELECTIVITY ANALYSIS

The response time is also a vital parameter of the sensor, which was calculated as the time required to decrease the I_{DS} from 10% to 90% of its base value after changing ion concentration. An enlarged image for response time calculation at 1 ppb has been shown in Figure 5.6, where the 10% decrement in I_{DS} was observed at 600.42 seconds, and 90% decrement was observed at 603.13 seconds [Nigam *et al.*, 2019a]. Hence, the response time of the sensor observed is 2.71 (~ 3) seconds at 1 ppb [Fan Ren and Pearton, 2011]. It is the shortest response time observed for Cd^{2+} ion detection using MPA-GSH functionalization.

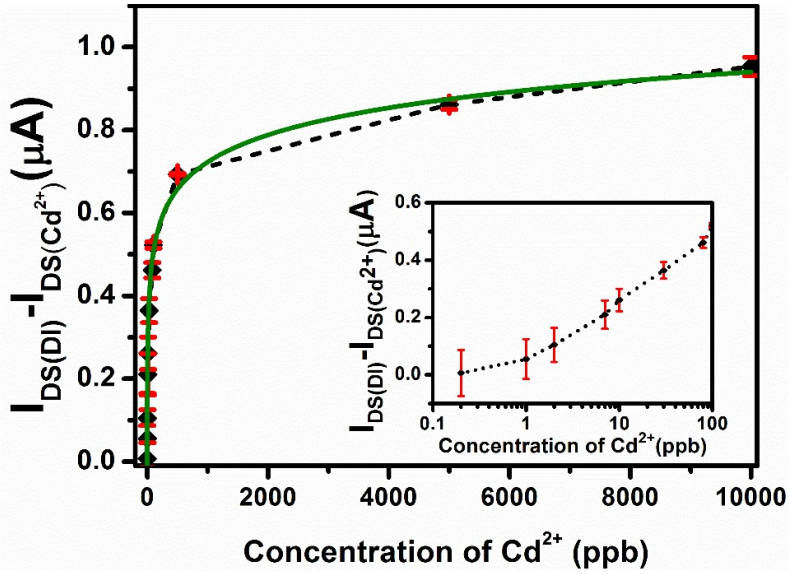

Figure 5.5: Calibration curve and response of the device with Cd^{2+} ion concentration (inset: response at the lower concentration of Cd^{2+})

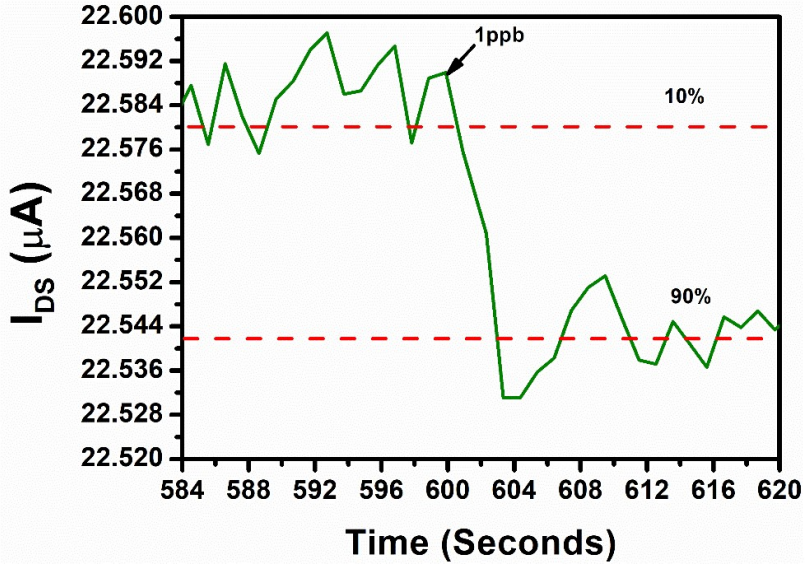

Figure 5.6: Response time of the sensor at 1 ppb Cd^{2+} concentration

To explore the selectivity of the MPA-GSH functionalized AlGaN/GaN HEMT sensor, the behavior of the sensor by separate solution technique was investigated in which it was exposed to various common heavy metal ions: Cr^{3+}, Cu^{2+}, Hg^{2+}, Ni^{2+}, Pb^{2+}, and Zn^{2+} with different ion concentrations from 10 ppb to 10 ppm. The relative current response and selectivity histogram are shown in Figure 5.7 (a) and Figure 5.7 (b), respectively. A generalized equation for all the heavy metals is given as in Eq. (5.3), which merely subtracts the average variation in I_{DS} with base current ($I_{DS(Blank)}$). In Figure 5.7 (a), the response of the Cd^{2+} metal ions compared with other heavy metal ions at different concentrations is shown.

$$I_{DS} = I_{DS(Blank)} - I_{DS(M^{n+}\,ions)} \tag{5.3}$$

Here, the $I_{DS(Blank)}$ is a base current for the $I_{DS(M^{n+}ions)}$ measured at different metal ion concentrations, M is the heavy metal (Cd, Cr, Cu, Hg, Ni, Pb, Zn), and n is the number of charges

on metal ions (n = 1, 2, 3). The selectivity of the HEMT sensor due to a change in the ion concentration can also be expressed through the calculation of the normalized drain current [Ruan *et al.*, 2015]:

$$I_{DSN}(\%) = \frac{I_{Blank} - I_{ion}}{I_{Blank}} \times 100 \quad (5.4)$$

where I_{ion} and I_{Blank} refer to the drain currents in the different metal ion solutions and blank, respectively. The response of the sensor with this normalized current has been observed, and the corresponding histogram is shown in Figure 5.7(b). The response of the sensor for Cd^{2+} ions are compared with the responses of the sensor to other heavy metal ions. The significant difference in responses is due to the fact that carbonyl and sulfhydryl groups of GSH favor the binding with Cd^{2+} ions. The response showed some interference of Cu^{2+}, Hg^{2+}, and Pb^{2+} ions in the selectivity analysis. It is because the Pb^{2+} and Hg^{2+} ions make the linear bonds with GSH, whereas the GSH makes tetrahedral $(GS)_4Cd$ complex with Cd^{2+} that have more net negative charges than GS-Hg-SG and GS-Pb-SG [Guo *et al.*, 2014; Pei *et al.*, 2011]. The observed response for Cu^{2+} is also not surprising because of the consideration of MPA-GSH functionalized gate contact for detecting metal ions. Cu shows a good affinity towards the MPA-GSH functionalizing layers, which competes with Cd for binding sites on MPA-GSH [Chow *et al.*, 2005]. Hence, the MPA-GSH functionalized AlGaN/GaN HEMT sensor shown good selectivity for Cd^{2+} ion detection with some interference of Cu^{2+}, Hg^{2+}, and Pb^{2+} ions. Here, the limit of detection of the metals Cr, Cu, Hg, Ni, Pb, Zn is calculated as 16.1 ppb, 9.45 ppb, 7.1 ppb, 1.13 ppm, 5 ppb, and 20 ppb, respectively. The limit of detection obtained for Cd was 0.255 ppb, which is very less than the other interfering metal ions[Nigam *et al.*, 2019a]. The comparative analysis of the limit of detection of other metal ions showed the effectiveness of the sensor in terms of selectivity.

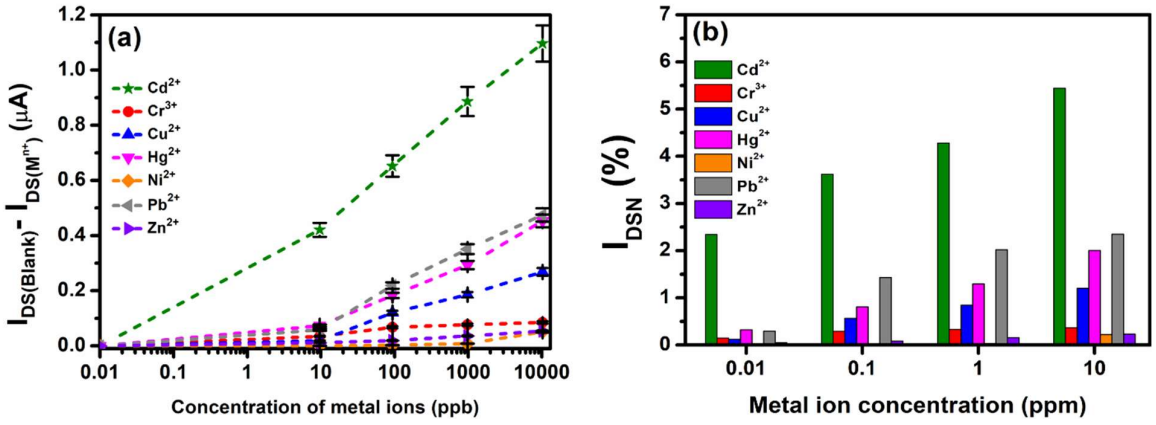

Figure 5.7: Selectivity observation of the sensor (a) Comparison of the response of the Cd^{2+} ions with different heavy metal ions. Here, M is the heavy metal (Cd, Cr, Cu, Hg, Ni, Pb, Zn), and n is no. of charges on metal ions (n= 1, 2, 3). (b) Selectivity histogram of the developed sensor with Cd^{2+} and other metal ions by normalized current calculation.

5.8 EFFECT OF pH ON THE SENSING RESPONSE OF THE SENSOR

In this section, the influence of pH on the sensing response of the sensor was observed. Here, the maximum concentration of Cd^{2+} ions (10 ppm) was taken for this analysis and varied the pH from 4 to 10. Figure 5.8 shows the response of the sensor at different pH with 10 ppm Cd^{2+} ion concentration. The response was observed as a difference between I_{DS} of reference solution with I_{DS} at 10 ppm Cd^{2+} ion concentration. The pH of the reference solution and the Cd^{2+} ion solution was kept constant during observation in the response at a particular pH. It was observed that the sensor showed the highest sensitivity at pH 7 as compared to other pH values. The response at lower concentration (more acidic conditions) was decreased due to the protonation of ligands of GSH. Therefore, they lose their capacity to form the complex with Cd^{2+} ions,

whereas, at higher pH values, the hydroxyl ions of the solution react with Cd^{2+} ions, which form Cd $(OH)_2$ and thereby reduces the sensitivity [Ensafi *et al.*, 2009]. It has also been observed that at pH more than 6.5, an increase in the binding of amino and carboxyl groups occurs, increasing the sensitivity of Cd^{2+} ions at pH 7 [Chow *et al.*, 2005].

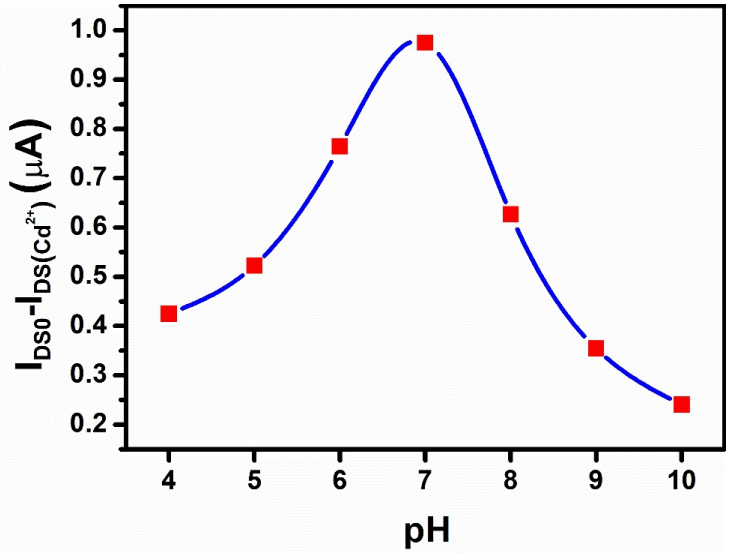

Figure 5.8: Influence of the pH on the response of the sensor at 10ppm Cd^{2+} ion concentration.

5.9 RECOVERY, REPEATABILITY, AND REPRODUCIBILITY OF THE SENSOR

5.9.1 Recovery of the Sensor

After the detection of Cd^{2+} or other metal ions, the MPA-GSH functionalized layer at the gate region of the device was cleaned by applying V_{GS} = +0.5 V at the gate terminal in 0.1 M $HClO_4$ for 120 s so that bound metal ions at the gate region were removed. Subsequently, the device was checked in a metal ion free buffer solution (blank) compared to the reference current [Nigam *et al.*, 2019a]. Figure 5.9 shows the response and recovery of the sensor. The table-5.1 explains the optimization of the recovery time of the sensor. Here, $I_{DS(Blank)}$ is the drain to source current of the reference, measured before applying Cd^{2+} ion solution, and $I_{DS\ (after\ recovery)}$ refers to drain to source current measured on the buffer solution with no Cd^{2+} ion concentration after applying $HClO_4$ for a particular recovery time. It has been observed that at 120 seconds, the sensor showed 99.61% recovery [Nigam *et al.*, 2019a].

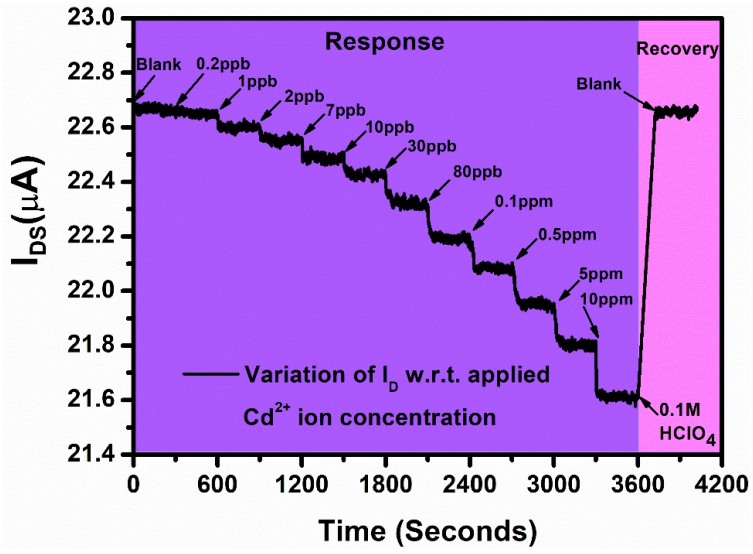

Figure 5.9: Response and recovery of the Cd^{2+} ion sensor.

Table 5.1: Optimization of Recovery Time

S. No.	$I_{DS\ (Blank)}$	$I_{DS\ (After\ Recovery)}$	Recovery Time (Seconds)	Recovery (%)
1	22.635 µA	21.884 µA	30	27.44
2	22.626 µA	22.232 µA	60	61.60
3	22.631 µA	22.455 µA	90	82.93
4	22.633 µA	22.629 µA	120	99.61

5.9.2 Repeatability of the Sensor

Repeatability of the sensor is an important parameter as it defines how much time the sensor gives the same response under the same conditions. Thus, the repeatability of the sensing response was performed under the same operating conditions and is shown in Figure 5.10. It was observed that the sensor possesses excellent repeatability behavior.

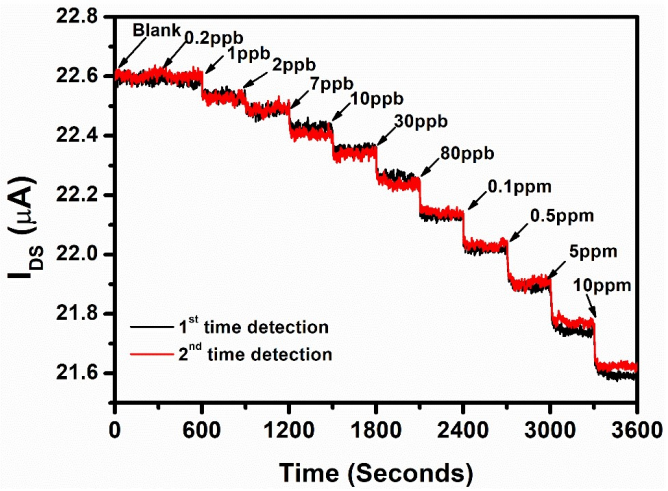

Figure 5.10: Repeatability behavior of the Cd^{2+} ion sensor.

5.9.3 Reproducibility of the Sensor

The reproducibility of the sensor was achieved by the fabrication of another sensor using the same process as described in previous sections and observed the sensing response on it. The comparative analysis of the responses of both the devices is shown in Figure 5.11, and it can be observed that both the sensors showed similar responses for each concentration. The slight variation in the current in the device can be due to the internal resistance of the device.

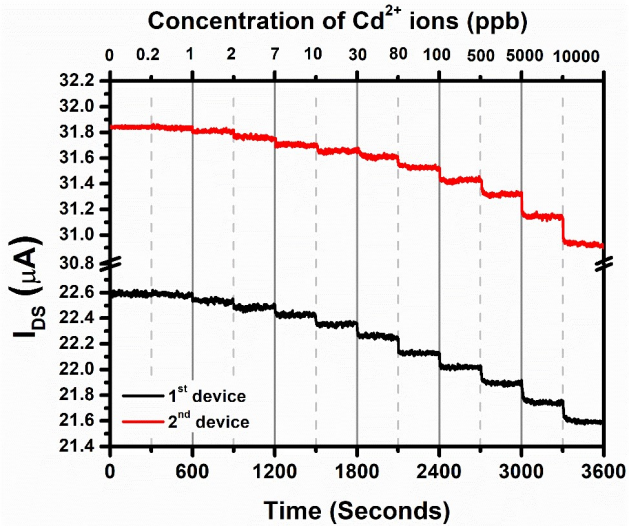

Figure 5.11: Reproducibility of the developed Cd^{2+} ion sensor.

5.10 SENSING MECHANISM OF THE DEVELOPED SENSOR FOR Cd^{2+} IONS DETECTION

The proposed sensing mechanism of the sensor has been shown in Figure 5.12. Since GSH is a strong detoxification reagent for Cd^{2+} ions, therefore, it can bind with Cd^{2+} ions efficiently [Guo *et al.*, 2014]. By considering this fact, the Au gate terminal surface was functionalized by MPA-GSH. The MPA has mercaptan (a thiol) that contains sulfur (S) [Chow *et al.*, 2005]. When the MPA layer was formed on the active gate region of the device, the Au makes the bonding with S, as shown in Figure 5.1 [Chen *et al.*, 2008; Kang *et al.*, 2007]. This Au-S bonding has been reported previously using X-ray photoemission spectroscopy (XPS) [Kang *et al.*, 2007]. The carboxyl group of the MPA provides the attachment of GSH by carbodiimide coupling [Chow *et al.*, 2005]. This process forms the bonds between GSH-MPA and Au during the functionalization process on the gate of HEMT, as shown in Figure 5.1. Previously, the binding of Cd with Glutathione was demonstrated using the colorimetric approach with gold nanoparticle (AuNp) and by cyclic voltammetry approach on Au and Hg electrodes [Chow *et al.*, 2005; Díaz-Cruz *et al.*, 1999; Guo *et al.*, 2014]. In these processes, mononuclear and dinuclear complexes like $[Cd(GSH)_x]^{n-}$ (x=1–4) and $[Cd_2(GSH)_y]^{n-}$ (y=2–4), respectively have been formed [Chow *et al.*, 2005; Díaz-Cruz *et al.*, 1997; Mah and Jalilehvand, 2010; Pei *et al.*, 2011] where n is the number of charge on the Cd-GSH complex. The coordination chemistry of Glutathione with Cd has been studied appropriately [Aliakbar Tehrani *et al.*, 2012; Chow *et al.*, 2005; Díaz-Cruz *et al.*, 1997, 1999; Kadima and Rabenstein, 1990] as the affinity of thiol groups with GSH is essential for the sensing of Cd^{2+} ions. GSH has a maximum of eight possible active sites: one sulfhydryl, one amino, two carboxyls, two pairs of carbonyl and amide donors [Aliakbar Tehrani *et al.*, 2012; Chow *et al.*, 2005; Zhou *et al.*, 2014] in which the sulfhydryl group of GSH always binds Cd preferentially [Guo *et al.*, 2014; Mah and Jalilehvand, 2010].

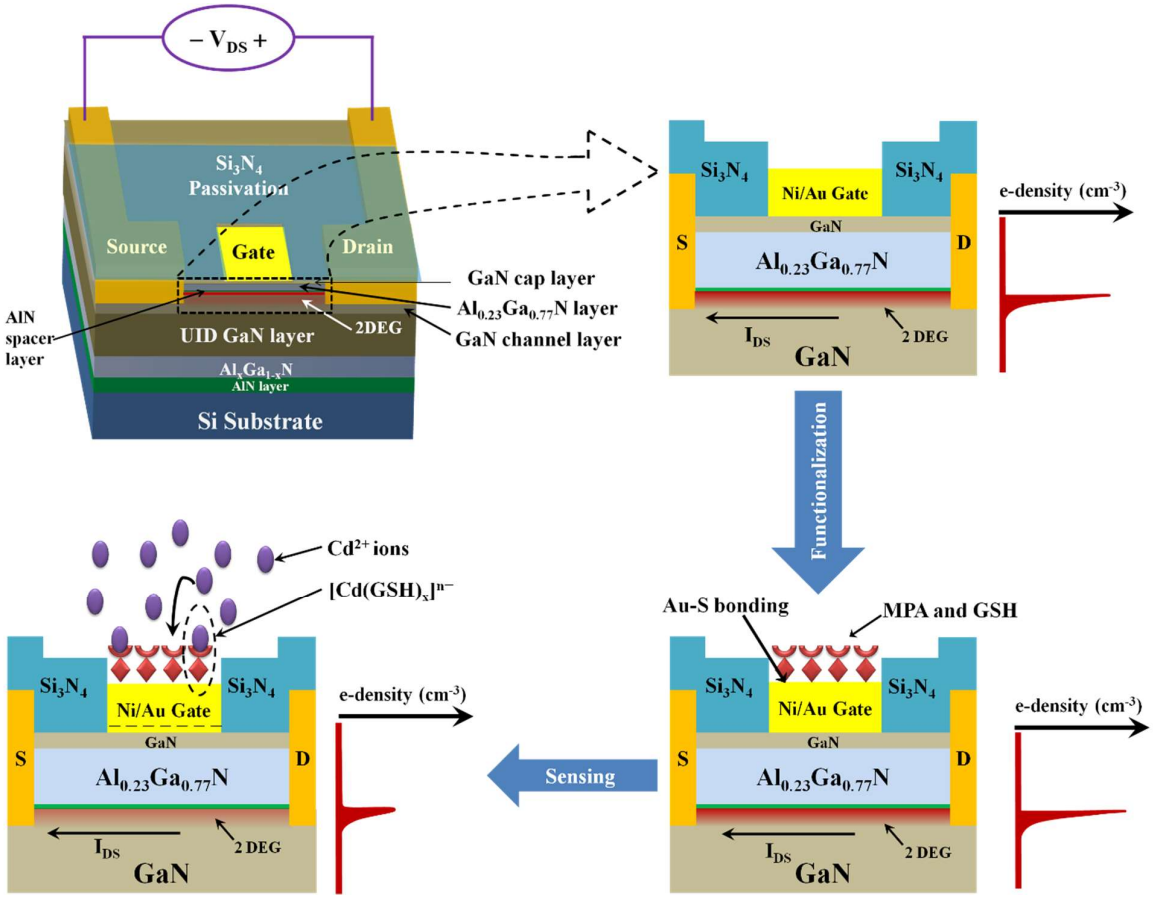

Figure 5.12: Mechanism of MPA-GSH functionalized Au gated AlGaN/GaN HEMT sensor for Cd^{2+} ion detection

After the functionalization of the device, when Cd^{2+} ions interact with the functionalized gate surface of the AlGaN/GaN HEMT, it forms the complex with GSH via sulfhydryl and carboxyl group. This complex formation process of Cd with GSH is called as detoxification of Cd [Mah and Jalilehvand, 2010]. The formed Cd-GSH complex has overall net negative charges [Guo *et al.*, 2014; Mah and Jalilehvand, 2010; Pei *et al.*, 2011] provide the negative surface potential on the active gate region that reduce the overall gate potential (V_G) of the device [Nigam *et al.*, 2019a]. Due to this, the charge density of 2DEG decreased as explained by Eq. (5.5) [Jia *et al.*, 2016], and hence drain current (I_{DS}) reduces by Eq. (5.1).

$$n_S = \frac{\varepsilon_n}{qd}(V_G - V_T - V(x)) \tag{5.5}$$

where q is the charge of the electron, and V(x) is channel potential.

5.11 COMPARISON OF THE DEVELOPED SENSOR OVER OTHER ION SENSORS

The comparison of the sensor with other conventional processes is shown in Table 5.2. It shows that the proposed sensor is the fastest among the conventional processes as they have a prolonged response time of 10 or more than 10 minutes. The proposed sensor has also shown a faster response than other HEMT based ion sensors. The detection limit of the device is 0.255 ppb, which is very less compared to other conventional processes. This lower detection limit was attributed due to the MPA-GSH functionalization over gate of AlGaN/GaN HEMT. The large electron density in the 2DEG of the AlGaN/GaN HEMT is induced by piezoelectric and spontaneous polarization effects. Because of 2DEG, there are positive counter charges induced at the surface. Any slight changes on the surface alter the concentration of the 2DEG [Chen *et al.*, 2008; Chu *et al.*, 2010]. In other words, the conductivity of the 2DEG channel is highly sensitive to the surface charges [Myers *et al.*, 2013]. This property of AlGaN/GaN HEMTs makes them highly sensitive heavy metal ion sensors.

Table 5.2: Comparison of Proposed Sensor with Previously Reported Sensors

Functionalizing Material	*Analyte (ions)*	*Process*	*LoD (ppb)*	*Sensitivity (μA/ppb)*	*Response Time*	*References*
MPA-GSH	Cd^{2+}	Functionalization on AlGaN/GaN HEMT	0.255	0.241	~ 3 s	This work
GSH on AuNP	Cd^{2+}	Colorimetric	562 3.37	— —	— 17 min.	[Asadnia *et al.*, 2016; Guo *et al.*, 2014]
MPA-GSH	Cd^{2+}	Electrochemical	0.56	—	10 min.	[Chow *et al.*, 2005]
Screen Printed Electrode	Cd^{2+}	Electrochemical	2.9	0.051	2 min.	[Güell *et al.*, 2008]
Cu/Nafion/ Bi electrode	Cd^{2+}	Electrochemical	0.68	0.1802	2 min.	[Legeai and Vittori, 2006]
Bi/ TRGO/ Au electrode	Cd^{2+}	Electrochemical	1	0.05±0.01	2.5 min.	[Xuan *et al.*, 2016]
Ion Imprinted polymer	PO_4^{3-}	Functionalization on AlGaN/GaN HEMT	1.97	0.003191	—	[Jia *et al.*, 2016]
AuNP Amalgam	Cd^{2+}	Screen-printed carbon electrodes	2.6	—	60 s	[Zhang *et al.*, 2010]
PVC based ion-sensitive membrane	Hg^{2+}	Functionalization on AlGaN/GaN HEMT	27	—	< 5 s	[Wang *et al.*, 2007]
Thioglycolic acid	Hg^{2+}	Functionalization on AlGaN/GaN HEMT	4	—	<5 s	[Chen *et al.*, 2008]

5.12 CONCLUSION

In this chapter, the AlGaN/GaN HEMT ion sensor functionalized with MPA and GSH was fabricated successfully. The detection of Cd^{2+} ions was observed by monitoring the change in the drain current of the HEMT. The sensor showed good sensitivity and an excellent response time of ~ 3 seconds. The sensitivity of the sensor is 0.241 μA/ppb. The detection limit observed is 0.255 ppb, which is less than the drinking water standards of the WHO (3 ppb). The sensor also exhibits good selectivity over other heavy metal ions. A little interference of Cu^{2+}, Hg^{2+}, and Pb^{2+} was detected; however, the effects of Cr^{3+}, Ni^{2+}, and Zn^{2+} were negligible. The device also showed good repeatability and reproducibility. Thus, the AlGaN/GaN HEMT based sensor offers a promising way for real-time, efficient, and fast detection of Cd^{2+} ions.

…